LATERAL DIFFUSION OF LIPIDS AND GLYCOPHORIN IN SOLID PHOSPHATIDYLCHOLINE BILAYERS

The Role of Structural Defects

H. G. KAPITZA AND D. A. RÜPPEL
Abteilung für Biophysik, Universität Ulm, D-7900 Ulm, Federal Republic of Germany

H.-J. GALLA
Institut für Organische Chemie und Biochemie, Technische Hochschule Darmstadt, D-6100 Darmstadt, Federal Republic of Germany

E. SACKMANN
Physics Department E/22, Technische Universität München, D-8046 Garching bei München, Federal Republic of Germany

ABSTRACT The lateral mobility of the lipid analog *N*-4-nitrobenzo-2-oxa-1,3 diazole phosphatidylethanolamine and of the integral protein glycophorin in giant dimyristoylphosphatidylcholine vesicles was studied by the photobleaching technique. Above the temperature of the chain-melting transition (T_m = 23°C), the diffusion coefficient, D_p, of the protein [$D_p = (4 \pm 2) \times 10^{-8}$ cm^2/s at 30°C] was within the experimental errors equal to the corresponding values D_L of the lipid analog. In the $P_{\beta'}$ phase the diffusion of lipid and glycophorin was studied as a function of the probe and the protein concentration. (*a*) At low lipid-probe content ($c_L < 5$ mmol/mol of total lipid), ~20% of the probe diffuses fast ($D \approx 10^{-8} - 10^{-9}$ cm^2/s), while the mobility of the rest is strongly reduced ($D < 10^{-10}$ cm^2/s). At a higher concentration ($c_p \sim 20$ mmol), all probe is immobilized ($D < 10^{-10}$ cm^2/s). (*b*) Incorporation of glycophorin up to c_p = 0.4 mmol/mol of total lipid leads to a gradual increase of the fraction of mobile lipid probe due to the lateral-phase separation into a pure $P_{\beta'}$ phase and a fraction of lipid that is fluidized by strong hydrophilic lipid-protein interaction. (*c*) The diffusion of the glycophorin molecules is characterized by a slow and a fast fraction. The latter increases with increasing protein content, which is again due to the lateral-phase separation caused by the hydrophilic lipid-protein interaction. The results are interpreted in terms of a fast transport along linear defects in the $P_{\beta'}$ phase, which form quasi-fluid paths for a nearly one dimensional and thus very effective transport. Evidence for this interpretation of the diffusion measurements is provided by freeze-fracture electron microscopy.

INTRODUCTION

Translational and rotational diffusion processes (1) of lipids and proteins are of considerable interest to investigators attempting to understand the function of cell membranes. For example, the lateral mobility may be of importance in coupling components of enzyme-acceptor systems, where the reaction rates could be diffusion limited (2).

In the last decade several spectroscopic techniques have been developed to measure the lateral diffusion coefficients of membrane constituents. Spin-lattice relaxation measurements (3) or experiments using pulsed magnetic-field gradients (4) were performed to investigate the lateral diffusion by NMR-spectroscopy, which has the advantage that no probe molecules have to be incorporated into the lipid bilayer. One type of the techniques that use spectroscopic probes is based on the analysis of controlled bimolecular reactions that include exchange interaction between spin probes (5–7), the excimer formation (8), and the triplet-triplet annihilation (9). The excimer-formation technique leads to an interpretation of the lateral diffusion in terms of a free volume model (10, 11). A second set of probe techniques is based on the measurement of influx of labeled molecules into a predetermined area of a lipid bilayer. The fluorescence-correlation technique reviewed in a recent article (12) is applicable to measure lateral diffusion coefficients $D > 10^{-8}$ cm^2/s (13–15) in accordance with the techniques thus far summarized. More recently, the technique of fluorescence recovery after photobleaching (FRAP) to measure the mobility of fluorescent-labeled lipid or protein probes has become a powerful tool for experimentation. Numerous studies have been performed on model membranes and living cells (16).

Fluorescent-lipid probes (17–19) and proteins (20–24) have been incorporated into bilayer membranes and their diffusion measured. Moreover, the lateral diffusion coefficients of natural proteins in biomembranes, e.g., rhodopsin in the photoreceptor cell, have been determined (25). To summarize, diffusion coefficients between 10^{-10} cm^2/s and 10^{-7} cm^2/s can be easily measured by the photobleaching technique. This range includes the diffusion below and above the lipid-phase transition temperature in artificial bilayer systems. One advantage of the FRAP technique is the applicability of the method to measure average diffusion coefficients below the phase transition even if the membrane system exhibits an inhomogeneous distribution of fluid and rigid domains.

The present work is part of a study on the interaction of glycophorin with lecithin bilayers (26). The lateral diffusion of a lipid analogue and of a protein was systematically investigated below the lipid-phase transition temperature focusing on the $P_{\beta'}$ phase. In particular, we were interested in two questions: (*a*) do the defects of the crystalline phases play an essential role for the lateral mobility, and (*b*) how is this property influenced by the incorporation of increasing amounts of small or macromolecular solute molecules? To answer these questions the lateral diffusion coefficients were measured as function of the lipid probe and of the glycophorin content. Our finding of the ratio of a fast and a slowly diffusing component, which depends critically on the solute concentration, demonstrates the important role that defects play in the transport properties in crystalline phases. Moreover, we provide evidence that lateral diffusion measurements may yield valuable information concerning the microstructure of bilayer membranes and the lipid-protein interaction. Our experiments were performed on large vesicles with thin shells composed of less than about 10 bilayers. These systems were used to minimize the bilayer-bilayer interaction that may influence the protein lateral diffusion.

MATERIALS AND METHODS

Lipids, Protein Preparation, and Membrane Reconstitution

Dimyristoylphosphatidylcholine (DMPC) was obtained from Fluka, Neu-Ulm, Federal Republic of Germany; N-4-nitrobenzo-2-oxa-1,3-diazole-phosphatidylethanolamine (NBD-PE) was a commercial product of Avanti Biochemicals (Birmingham, AL). Glycophorin was isolated as described earlier (26) and purified on a wheat germ lectin-Sepharose column (Sepharose 6MB, Pharmacia Uppsala, Sweden). Glycophorin was labeled with fluoresceine-isothiocyanate (26). From optical density measurements, we found an average of one dye molecule per protein molecule.

Glycophorin was incorporated into DMPC bilayers according to McDonald and McDonald (27). The lipid (including the NBD-PE probe) was dissolved in methanol/chloroform (3:1, vol/vol). To this solution appropriate amounts of an aqueous dispersion of glycophorin were added and the mixture was slightly sonificated. The protein or the fluorescent lipid dye concentration is given in millimoles per mole of unlabeled lipid.

For the FRAP experiments 50 μg of lipid and protein in 50 μl of solvent was deposited on carefully purified microslides. The solvent was evaporated for ~1 hr at 35°C. Then 100 μl of phosphate buffer (pH 7.5) was added. After a wait of ~1 min, a cover glass was put on the sample. The gap between cover glass and microslide was sealed to prevent water evaporation (28). The homogeneity of the lipid film on the microslide was checked by the fluorescence image in a light microscope.

METHODS

Diffusion coefficients of the lipid, D_L, or protein, D_P, were measured by the FRAP technique introduced by Peters et al. (29), who used the evaluation procedure of Axelrod et al. (30). The apparatus was designed to allow measurements at high magnification and was described previously (28,31). For the experiments, vesicles (up to 50-μm diam) that appeared homogeneous as judged from the distribution of fluorescence intensity were selected.

The measurement of the degree of polarization was performed with the same microscope (Axiomat; Carl Zeiss, Inc., Oberkochen, Federal Republic of Germany) as the FRAP experiments. Fluorescence excitation was performed with a mercury high-pressure lamp in combination with narrow-band interference filters. For excitation with polarized light, a reflecting objective equipped with a polarizer was used. The emission was observed through the objective and was separated from the excitation light by a second set of interference filters. Its polarization was analyzed with a second polarizer. With crossed polarizer and analyzer, the extinction of the excitation light was 1:500.

Samples for electron microscopy were prepared as follows: ~20-μm-thick layers of the vesicle suspension were brought between gold-plates (100-μm thickness; 5-mm diam) and were rapidly frozen by dipping into freon kept at −155°C. Before this, the samples were equilibrated at the desired temperature for 16 h before freezing. The freezing rate was ~10^4 K/s (32). Freeze fracturing was performed in a BAF 400 D device (Balzers, Hudson, NH) at −120°C and 10^{-7} mbar. The fracture faces were shadowed without additional etching (water sublimation) under 45°C with platinium/carbon up to a thickness of 3 nm (33).

RESULTS

Lipid Diffusion in the $P_{\beta'}$ Phase of DMPC Bilayers

The lateral diffusion of the lipid analogue NBD-PE has been investigated by the photobleaching FRAP technique in DMPC bilayer vesicles. The temperature dependence of the lateral diffusion coefficient of the lipid probe, D_L, is shown in Fig. 1 *A* and *B* for different probe concentrations.

At low probe concentration (C_L = 0.5 mmol/mol unlabeled lipid), D_L decreases exponentially with decreasing temperature above the main lipid-phase transition temperature (T_m = 23°C for DMPC). Upon lowering the temperature below the main transition temperature the coefficient of the lateral diffusion decreases sharply from 2×10^{-8} cm^2/s to 2×10^{-9} cm^2/s. D_L is nearly constant between the main and the pretransition and exhibits a second sharp decrease to $D < 10^{-10}$ cm^2/s at the pretransition temperature (T_P = 14°C for DMPC). One remarkable result is the rather high lipid mobility of $D_L = 2 \times 10^{-9}$ cm^2/s in the $P_{\beta'}$ phase, which is more characteristic for a fluid than for a solid phase.

A completely different behavior was found at higher lipid-dye concentration (C_L = 20 mmol). At $T > T_m$ we

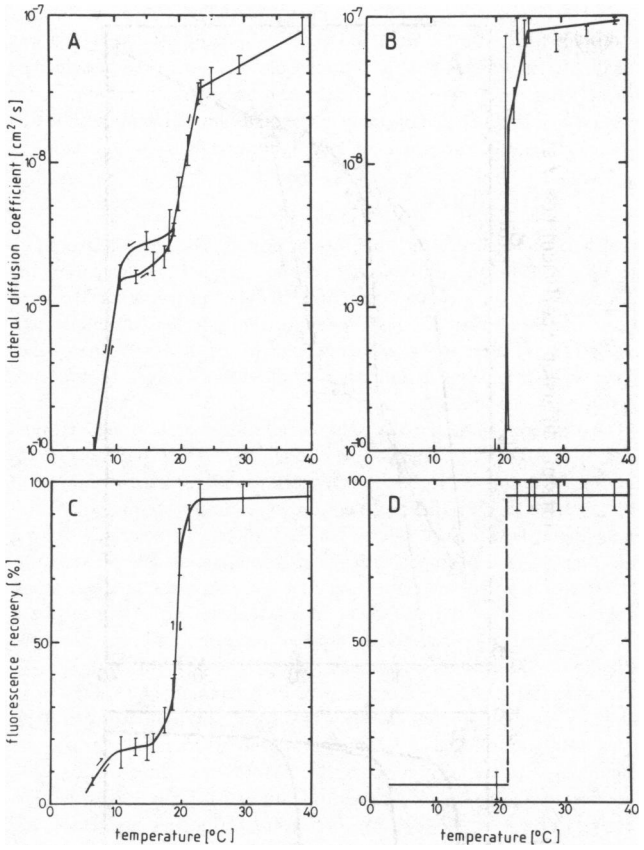

FIGURE 1 Diffusion coefficients D_L of the lipid probe NBD-PE in DMPC bilayer membranes are given as function of temperature for two different probe concentrations. (*A*) C_L = 0.5 mmol of NBD-PE per mol DMPC; (*B*) C_L = 20 mmol. The relative amount of the fast-diffusing lipid is given in terms of percentage of recovery (R %). R is plotted vs. temperature for *C*: C_L = 0.5 mmol and (*D*) C_L = 20 mmol. The large error bar in *B* at 22°C indicates the simultaneous observation of two values of D_L between 2×10^{-8} and 2×10^{-10} cm²/s.

observed a relatively high diffusion coefficient of 8×10^{-8} cm²/s without a significant temperature dependence. At 22°C two diffusing species are simultaneously observed with D_L values of 2×10^{-10} cm²/s and 2×10^{-8} cm²/s, respectively. With further decreasing temperature, below 20°C, the lateral diffusion coefficient drops within a very sharp temperature interval to a value $D_L < 10^{-10}$ cm²/s. Simultaneously all lipid becomes immobilized (Fig. 1 *B*) below this temperature.

As already mentioned, it was necessary in some cases to divide the measured lateral diffusion into a fast ($D > 10^{-9}$ cm²/s) and a slow ($D < 10^{-10}$ cm²/s) component. The relative amounts of the fast diffusing component is given in Fig. 1 *C* and 1 *D* in terms of percentage of fluorescence recovery (R). The temperature dependence of R shows a remarkable difference for the low (C_L = 0.5 mmol, Fig. 1 *C*) and the high (C_L = 20 mmol, Fig. 1 *D*) probe concentration. In the first case we clearly observe that a fraction of 20% of lipid probe diffuses rapidly in the crystalline $P_{\beta'}$ phase ($D_L = 2 \times 10^{-9}$ cm²/s). At C_L = 20 mmol, however, the percentage of recovery drops practically to zero at $T \leqq 20$°C. This again demonstrated the complete immobilization ($D_L < 10^{-10}$ cm²/s) of the lipid probe below 20°C.

Fluorescence Depolarization Measurements

Microfluorimetric depolarization measurements that use the NBD-PE lipid analogue incorporated into thin-walled DMPC vesicles were performed at low dye concentration (C_L = 0.5 mmol). The experimental curve shown in the upper part of Fig. 2 exhibits three regions where the degree of polarization, P, decreases linearly with increasing temperature but with different slopes. Remarkable is the rather steep decrease of P between 15 and 22°C, where the $P_{\beta'}$ phase exists. Note that only a break in the P vs. T plot, but no further steplike decrease in P, could be observed at the main transition temperature. These findings show that the fluorophore (or the whole probe) is rather mobile just below the main transition. Inasmuch as P is an ensemble average of species with different rotational tumbling mobilities, the steep decrease in P at $T_P < T < T_m$ indicates that the fraction of fast-tumbling probes decreases at decreasing temperature. The lifetime of the fluorescence probe gently decreases from 8.5 to 7 ns over the whole temperature range and is thus not responsible for the changes in the degree of polarization.

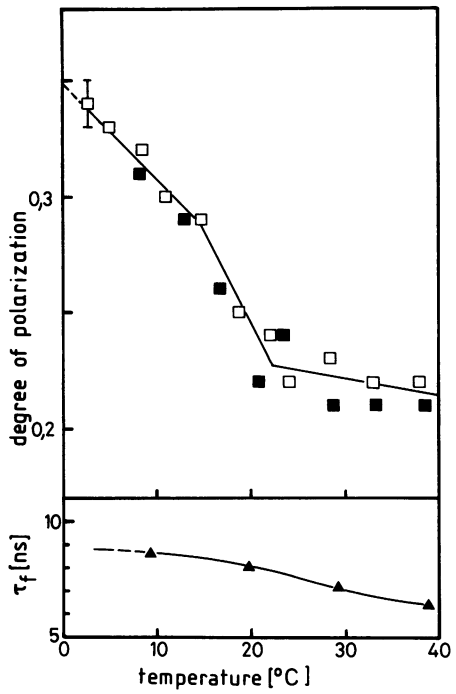

FIGURE 2 Temperature dependence of the degree of polarization, P, of the probe NBD-PE incorporated into DMPC membranes. The probe concentration was C_L = 0.5 mmol/mol lipid. The degree of polarization was measured with a micro fluorimeter. The lower part displays the NBD-PE fluorescence lifetime as function of temperature again measured microscopically.

Lipid Diffusion in the Presence of Glycophorin

Again the fluorescent lipid analogue NBD-PE was used as dye molecule. The dye concentration was C_L = 0.5 mmol for all experiments. As shown in Fig. 3 *A* incorporation of glycophorin into DMPC bilayer vesicles drastically changes the lipid lateral diffusion below the main phase transition temperature, whereas no change could be observed in the fluid phase. In Fig. 3 *A* the temperature dependence of the lipid lateral diffusion in the absence of glycophorin (curve *a* taken from Fig. 1 *A*) is compared with curves obtained in the presence of 0.2 mmol (curve *b*) and 0.4 mmol (curve *c*) glycophorin per mol lipid. The corresponding fractions of the fast component given as percent recovery (%*R*) are shown in Fig. 3 *B*.

In the presence of 0.2 mmol glycophorin, the fast lateral diffusion of the lipid decreases exponentially with decreasing temperature down to the pretransition temperature. At 15°C, which is close to the pretransition temperature, the lateral diffusion coefficient is still $D_L = 2 \times 10^{-8}$ cm²/s, and the percentage, *R*, of fast fluorescence recovery amounts to *R* = 98%. Below the pretransition temperature, D_L drops to 10^{-9} cm²/s at 10°C. The fraction of fast recovery is *R* = 50%. Even at 5°C the lateral diffusion is only reduced to $D_L = 3 \times 10^{-10}$ cm²/s and 30% of the lipid is still mobile. At 0.4 mmol glycophorin per mole lipid (curve *c*), the downward deflection of the lipid lateral diffusion is shifted to lower temperatures. Even at 5°C, which is 10°C below the pretransition temperature, 90% of the lipid is able to diffuse almost as fast as in the fluid L_α phase, although one glycophorin molecule is surrounded by an average of 4,000 lipid molecules which are crystalline in the absence of protein. The results of the lipid diffusion in the presence of glycophorin are summarized in Fig. 4. The temperatures at which the diffusion coefficients exceed the limiting value, $D_L = 3 \times 10^{-8}$ cm²/s, or at which the limiting value drops below $D_L = 5 \times 10^{-9}$ cm²/s are plotted as function of glycophorin concentration for $C_P < 0.5$ mmol/mol lipid. Three regions are distinguishable. Region I covers lateral diffusion coefficients that are characteristic for a fluid phase. In region II mobile and immobile lipid fractions coexist. This region broadens with increasing glycophorin concentration. Region III covers the temperature-concentration range where the lipid lateral diffusion is mainly frozen in.

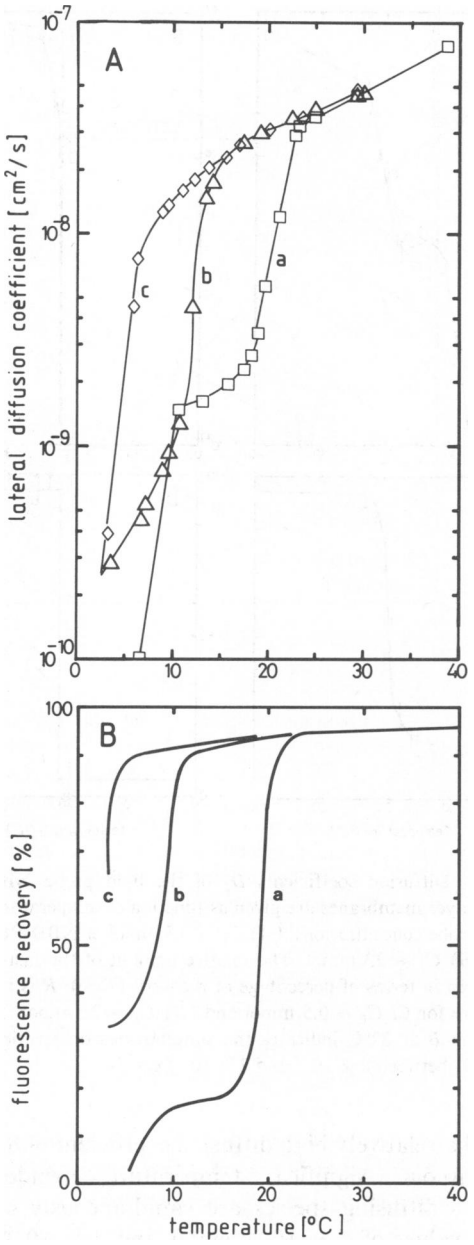

FIGURE 3 (*A*) Lateral diffusion coefficients, D_L, of the lipid probe NBD-PE in DMPC bilayers containing different amounts of glycophorine are given as function of temperature. Curve *a*, pure lipid bilayers; curve *b*, membrane preparations that contain 0.2 mmol glycophorin per mol lipid; curve *c*, 0.4 mmol glycophorin per mol lipid. (*B*) Fraction of fast-diffusing lipids (percentage of recovery, *R* %) as a function of temperature. Curve *a*, pure DMPC bilayers; curve *b*, DMPC bilayers containing 0.2 mmol glycophorin per mol lipid; curve *c*, 0.4 mmol glycophorin per mol lipid.

Lateral Diffusion of Glycophorin in DMPC Bilayers

Fluorescence-labeled glycophorin was incorporated as an integral protein into giant DMPC bilayer vesicles. The temperature dependence of the lateral diffusion coefficient, D_P, of the protein is given in Fig. 5 *A* and *B* for two small protein concentrations, C_P = 0.2 and C_P = 0.4 mmol/mol lipid. The corresponding curves of the percentage of fast recovery are shown in Fig. 5 *C* and *D*.

The results are good compared with those obtained for the lipid probe. The protein diffusion coefficient, D_P, decreases exponentially below the main-phase transition temperature of the lipid. Near the pretransition temperature, a fast ($D_P \sim 10^{-9}$ cm²/s) and a slow component ($D_P \sim 10^{-10}$ cm²/s) coexist. At C_P = 0.2 mmol and *T* = 15°C, for example, 50% of the protein was found to diffuse

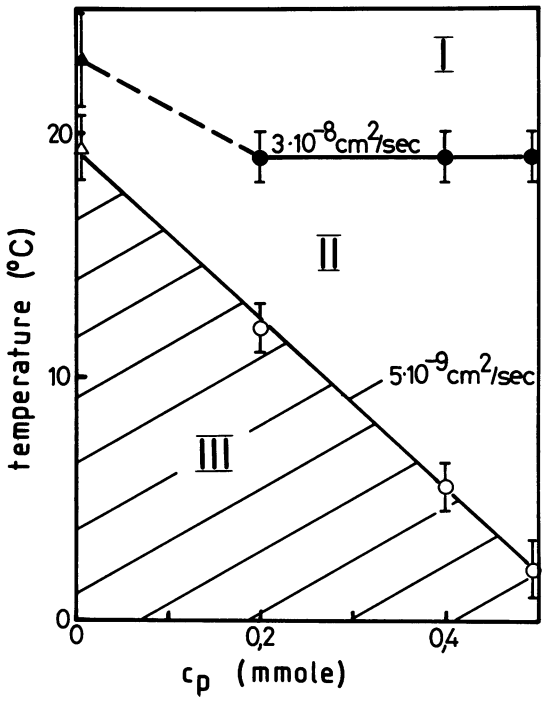

FIGURE 4 Temperature range for a fast and slow lateral diffusion of the NBD-PE probe as function of glycophorin concentration given in millimoles per mole lipid. Two arbitrary values $D_L = 3 \times 10^{-8}$ cm^2/s for a fast diffusion and $D_L = 5 \times 10^{-9}$ cm^2/s for a slow diffusion are taken as limiting values. Region I is characterized by diffusion coefficients that are found in the fluid L_α phase. Region II is a coexistence region of fluid and crystalline lipid. Region III corresponds to a mainly crystalline, lipid phase which may exhibit quasi-fluid paths formed by elongated defects.

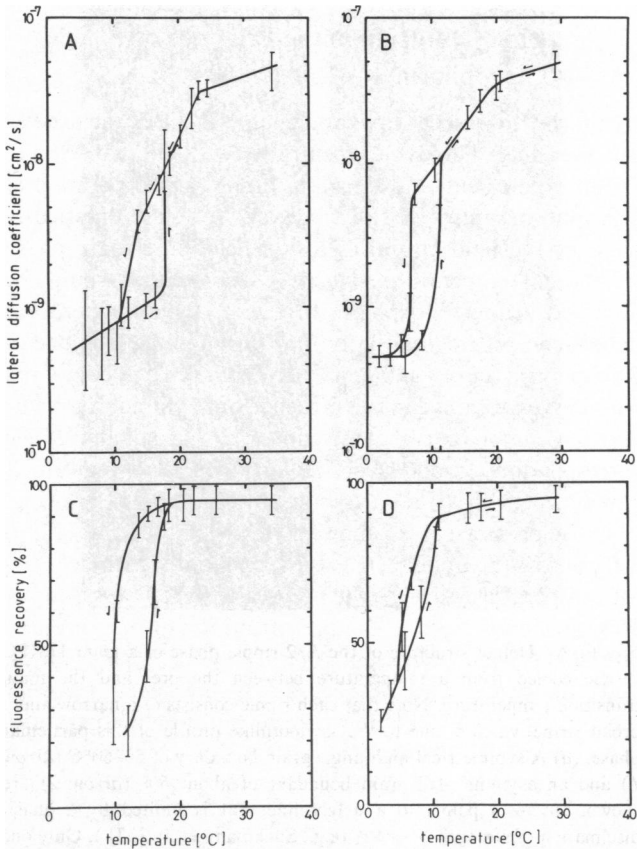

FIGURE 5 Lateral diffusion coefficient of fluorescence-labeled glycophorin in DMPC bilayers (*A*, *B*) and the corresponding percentage of the fast-diffusing component (*C*, *D*). The protein concentration was 0.2 mmol (*A*, *C*) or 0.4 mol (*B*, *D*) per mol lipid.

rapidly. Upon increasing C_P to 0.4 mmol glycophorin, the sharp drop in D_P is further shifted to lower temperatures. A 50% fraction of fast-diffusing glycophorin is reached at 10°C. Even at lower temperatures, down to 0°C, the lateral diffusion of the protein at this low protein content never becomes completely frozen in. Another remarkable result is the strong hysteresis between the heating and the cooling curves (direction marked by arrows in Fig. 5). Such a strong hysteresis was not observed if the diffusion of the lipid analogue NBD-PE was measured in the presence of an equal amount of (unlabeled) glycophorin.

Freeze-Fracture Microscopy of Pure and Doped DMPC Vesicles

Freeze-fracture micrographs of pure DMPC- and of glycophorin-containing vesicles are presented in Figs. 6–8. In Fig. 6 three types of extended defects are visible: (*a*) large-angle grain boundaries at which the ripples may be arranged in a symmetric (arrow 1 in Fig. 6 *a*) or in an asymmetric way (arrow 2 in Fig. 6 *a*); (*b*) small angle boundaries (Fig. 6 *b*); (*c*) line defects. The latter type of defect is shown on a larger scale in Fig. 7 *a*. It is due to the fact that the ripples of the $\Lambda/2$ phase exhibit a sawtoothlike profile and is thus characterized by a polarity in a direction perpendicular to the ripples. This form of the ripples is suggested by the finding that each ripple consists of a narrow and a broad stripe that is clearly visible in Fig. 7 *a*. A more direct proof has been given previously by a reconstruction of the three-dimensional surface profile (32, 33). At the line indicated by arrow 3 in Fig. 6 *a*, two regions of opposite orientation of the sawteeth meet, which is demonstrated by the fact that the order of the small and broad stripes of each ripple is reversed when the line is crossed in a direction perpendicular to the ripples. As was shown previously (33), the average planes of the two regions of opposite orientation form a roof. For this reason the lipid arrangement within the defects is expected to be strongly disordered.

Fig. 7 *b* demonstrates that the shape of the defects is very sensitive against small amounts of impurities. The vesicle of Fig. 7 *b* was prepared in the presence of the 20-mmol NBD-PE probe. Note that this is essentially the same probe as for the photobleaching experiment shown in Fig. 1 *B*. It is clear that the very long linear defects of the type shown in Fig. 7 *a* have shortened and are sometimes nearly reduced to point defects. This point has been extensively discussed by D. Rüppel (32).

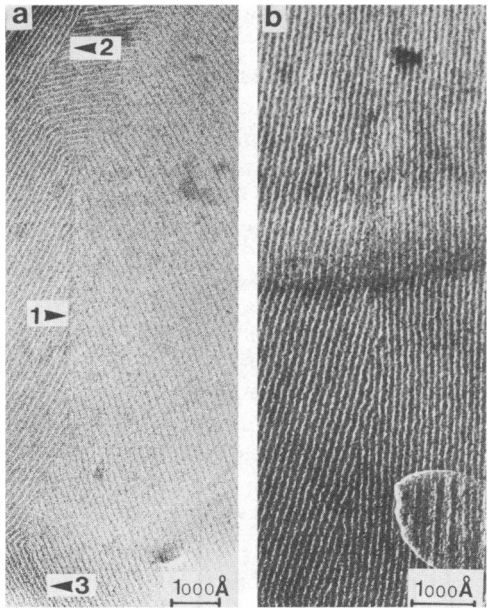

FIGURE 6 Defect structure of the $\Lambda/2$ ripple phase of a giant DMPC vesicle cooled from a temperature between the pre- and the main transition temperature. Note that each ripple consists of a narrow and a broad stripe which is due to the sawtoothlike profile of this particular phase. (*a*) A symmetrical high-angle grain boundary of 50–60°C (*arrow 1*) and an asymmetrical grain boundary of about 50° (*arrow 2*) are shown. *Arrow 3* points to a defect line that is limited by a quasi-disclination of strength $S = +½$ (e.g., Sackmann et al. [33]). Only one half of the defect is shown. (*b*) Symmetrical low-angle grain boundary of ~17°.

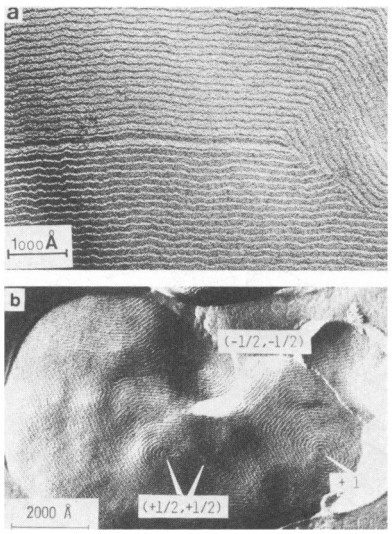

FIGURE 7 (*a*) Enlarged representation of a line defect of the $\Lambda/2$ ripple phase of a DMPC vesicle. The defect is limited by a pair of disclinations of strength $S = +½$. Only one-half of the line defect is shown. (*b*) Addition of small amounts of impurities leads to a shortening and broadening of the line defects. This vesicle contains 20 mmol of the fluorescent dye NBD-PE that was used in the photobleaching experiments. Closed defect pairs and a +1-defect are shown.

This very dramatic change of the defect structure is further demonstrated in Fig. 8 *a*, where the texture of the $P_{\beta'}$ phase is shown in the presence of small amounts of glycophorin. Obviously incorporation of a very small amount of protein leads to a shortening of the line defects and the ripples are occasionally closing up into loops. This provides very strong evidence that at very low concentrations the protein is preferentially contained in the more fluidized defects (26). Fig. 8 *b* shows that an increase of the protein concentration from 0.2 to 0.4 mmol has abolished the regular ripple structure, and that the bilayer now exhibits lateral-phase separation into patches of nearly pure DMPC and of lipid that is strongly distorted by the interaction with glycophorin. In a previous paper (26), we provided evidence that this phase separation is caused by strong hydrophilic interaction of the phosphatidylcholine head groups with the polysaccharide-containing head group of the protein. Thus in the limit of very low glycophorin concentrations, one protein head group interacts with ~300–400 lipid molecules (26).

DISCUSSION

Lateral Diffusion of Lipid Probes

Our value of the lipid lateral diffusion coefficients determined above the main-phase transition temperature of the lipid (e.g., $D_L = (5 \pm 1.5) \times 10^{-8}$ cm^2/s at $T = 30$°C in DMPC) agrees well with the results reported by other authors using the same technique (19, 34). The temperature dependence at a low probe concentration (e.g. 0.5

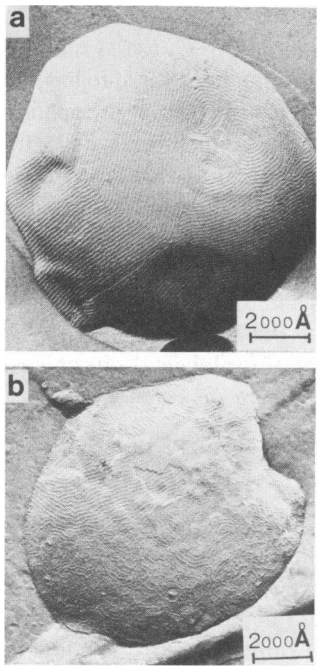

FIGURE 8 Electron micrograph of DMPC-vesicles containing (*a*) 0.2 mmol or (*b*) 0.4 mmol of glycophorin per mole lipid. Incorporation of low amounts of protein already leads to the formation of closed defect pairs. Note that the ripples form closed loops around the defects. Regions of irregular ripple structure appeared at 0.4 mmol glycophorin.

mmol NBD-PE per mol unlabeled lipid) shows a significant exponential course. From the slope of the log D vs. T plot, we have calculated an apparent activation energy of $E_a \sim 39$ kJ/mol, in good agreement with the results obtained by the excimer-formation technique (35). The exponential temperature dependence of the lateral diffusion supports an interpretation of the diffusion process by the free-volume model. In this model the apparent activation energy is a measure of the thermal expansion coefficient (10).

A remarkable finding is that, for high probe concentrations ($C_L = 20$ mmol), D_L does not depend appreciably on a temperature above T_m. This is due to the fact that in this case D_L is much higher just above T_m than at low probe concentrations. The most natural explanation is a disturbance of the lipid layer by the probe rather than a systematic error in the measurement.

Our main attention was focused on the temperature range between the pre- and the main transition. Two different diffusion coefficients were observed. The small value, $D_L < 10^{-10}$ cm^2/s, is characteristic for the gel state. ~80% of the lipid belongs to this class between 10 and 18°C. A fast diffusing fraction ($D_L > 10^{-9}$ cm^2/s) that comprises ~20% of the lipid is also present in this temperature range (e.g., Fig. 1 *A* and 1 *C*). The diffusion coefficient is about 10-fold smaller compared with those measured above the main phase transition temperature. The fast fraction exhibits another 20-fold decrease in D_L if the temperature is decreased below the pretransition. Here only a 5% fraction of lipid is able to perform fast lateral diffusion.

Earlier investigations (17, 34) of the lateral diffusion using the photobleaching technique reported slower values of D_L in DMPC multilayers in the $P_{\beta'}$ phase. However, these authors have analyzed their data by the assumption of only one characteristic time for the diffusion. Very recently Derzko and Jacobson (36) reported the coexistence of a fast and a slow component of the lipid lateral diffusion in the $P_{\beta'}$ phase. Because they used multibilayer systems of an inhomogeneous surface structure, defects between different bilayers are thought to be responsible for the fast lateral diffusion. In contrast, our results were obtained on homogeneous and thin-walled giant vesicles. Note that the interpretation given in the next paragraph, in terms of structural defects within the bilayer in $P_{\beta'}$ phase (ripple structure), should not be confused with macroscopic defects due to inhomogenities in the membrane preparation.

Role of Defect Structures for Lateral Diffusion in the $P_{\beta'}$ Phase

The existence of fast-diffusing species in the crystalline phase could be attributed to the formation of fluid domains. These may be caused by a disturbance of the lipid matrix by the probe molecules followed by lateral phase separation. However, this possibility can be ruled out because the fast-diffusing fraction decreases with increasing probe concentration.

Our diffusion measurements below the lipid main transition temperature led to the conclusion that the majority of the lipids is in the ordered state in the $P_{\beta'}$ phase. However, a coherent fluid-channel system that allows fast lateral transport over long distances must exist. Such fluid regions in the $P_{\beta'}$ phase were already postulated by Lee (37, 38). From the freeze-fracture results presented above (in Results, see Freeze-Fracture Microscopy) and in previous work (26, 32, 33, 39), we conclude that quasi-fluid channels for the fast lateral transport are formed by the elongated defects in the $P_{\beta'}$ phase.

According to Figs. 6–8, two types of elongated defects prevail: (*a*) wide- or small-angle grain boundaries, and (*b*) linear defects formed along lines where two regions of opposite orientation of the sawtoothlike ripple profile meet.

From three-dimensional surface reconstruction work (33) we know that the $\Lambda/2$ phase tends to form planar sheets and, consequently, the vesicles exhibit a polygonal shape. The edges of the polygons are formed by the linear defects, resulting in the distortion of the lipid-chain order along these lines, which may thus form quasi-fluid channels. Evidence for this conclusion was provided by the observation that solute molecules such as glycophorin are first dissolved within these defects. Incorporation of molecules into the crystalline regions will only occur if the defects are already filled up (26).

It is clear that the grain boundaries, especially those characterized by large angles, are expected to be more fluidlike compared with the linear defects. However, the linear defects are more numerous in vesicles of a diameter of some micrometers, and may thus play a dominant role for the fast lateral transport.

Note that quasi-fluid channels could also be formed along the maxima of the ripples of the so-called Λ phase, which often coexists with the $\Lambda/2$ phase (33). As noted previously (33), these ripples are actually formed by two $\Lambda/2$ ripples of an opposite orientation of the sawtoothlike profiles, and the structure at the maxima corresponds approximately to that of the defect lines.

Grain boundaries, especially those characterized by large angles, are regions of high lipid disorder where fast lateral diffusion may occur. These disordered regions within grain boundaries can be considered as nuclei where the melting process starts upon increasing the temperature to T_m. It appears that the melting of bilayers of large vesicles has to be considered a random process where small crystalline patches undergo a phase transition. Evidence for this is the gradual increase of the fraction of the fast-diffusing lipids and the increase of the D_L value of this species between 18° and 22°C (e.g. Fig. 1 *A*). Note that no sharp increase of D_L is observed at the phase-transition temperature of 23°C but only a break in the D_L vs. temperature plot.

The fluorescence polarization measurements given in Fig. 2 fit this interpretation. The degree of polarization decreases continuously (with increasing temperature) between the pre- and the main transition. The phase-transition temperature is only marked by a break in the P vs. T plot. This experiment yields an ensemble average of the degree of polarization distributed over a large lipid area. Thus a continuous decrease in P is expected if the number or the size of the fluid areas in the $P_{\beta'}$ phase increases.

Recently the lateral diffusion in the fluid L_α phase was explained in terms of a free-volume model (10), where a diffusive displacement of a molecule is controlled by the formation of a void within the bilayer membrane. We tend to explain the lateral diffusion in the $P_{\beta'}$ phase by the same model. However, the probability for the creation of free volumes is high only in the regions of the defect lines. It may indeed be as large as in the L_α phase. The slow diffusion has to be attributed to the crystalline phase and may proceed along interstitial sites or may be determined by the motion of vacancies.

Finally, we discuss our results in the light of a recent theory of Falkowitz et al. (40). Starting from a Landau-de Gennes theory, these authors concluded that the $P_{\beta'}$ phase may exhibit a periodic variation in lipid order and thus, in membrane fluidity, in a direction perpendicular to the ripple direction. Such a superstructure would indeed provide quasi-fluid paths for long-range diffusion. Such a structure would, however, lead to a very large number of paths, which contradicts our finding. We found that the fluid regions have already been saturated at rather small probe concentrations.

Another remarkable result is the temperature dependence of D_L observed at high lipid-probe concentrations (C_L = 20 mmol lipid analogue dye per mol DMPC). Here a steplike change of D_L is observed at the main transition temperature T_m (e.g., Fig. 1 *B* and *D*). Clearly the diffusion is completely frozen at temperatures below T_m. This finding is consistent with the given interpretation of a facilitated diffusion along defects and can be explained on the basis of the electron microscope observations. In pure DMPC bilayers the grain boundaries extend over long distances thus allowing for a fast long-range diffusion. The pattern of defects changes drastically in the presence of even small amounts of impurities. Incorporation of ~20 mmol of a solute per mol of DMPC (e.g., the NBD-PE probe) stabilizes the $\Lambda/2$ ripple structure. A rather regular, closed-defect pattern (e.g., Fig. 7 *b*) of pairs of $s = -\frac{1}{2}$ and $s = +\frac{1}{2}$ quasi-disclinations is formed. The pairs are connected by defect lines. These defect lines are shortened and may even form point defects (+1 or −1 defects) after incorporation of impurities. In this sense, high concentrations of probe molecules have to be regarded as impurities, and the dyes may be trapped within the defects. The diffusion may be fast within the closed structures. However, it would not allow a diffusion over large distances of some micrometers, which is probed by a photobleaching experiment.

Lipid Diffusion in the Presence of Glycophorin

The linear defect structure within the bilayer membrane is strongly affected by the incorporation of the integral protein glycophorin from human erythrocytes (26). Two electron microscope pictures of DMPC giant vesicles cooled from the $P_{\beta'}$ phase and containing 0.2 or 0.4 mmol glycophorin per mole lipid are shown in Fig. 8 *a* and *b*, respectively. The line defects in the $P_{\beta'}$ phase are considerably widened and are encircled by closed loops of ripples at 0.2 mmol. At 0.4 mmol glycophorin the defects are expanded and form large regions of irregular ripple structures. These domains coexist with patches of regular ripple structure, which correspond to almost pure DMPC in the gel state.

Our photobleaching experiments shown in Fig. 3 *A* and *B* may be explained by the assumption that the domains of irregular ripple structure are quasi-fluid. At 0.2 mmol, for example, half of the lipid undergoes fast lateral diffusion at 10°C (R = 50%). At 0.4 mmol of glycophorin the fraction of fast-diffusing lipid increases to 100% even at a temperature as low as 5°C. The temperature range (II in Fig. 4) where a coexistence of fast and slowly diffusing lipid is observed, is strongly broadened with increasing amounts of glycophorin. The upper and lower limits may thus be considered as liquidus and solidus lines of a DMPC/glycophorin phase diagram.

The remarkable point is that only 0.4 mmol of glycophorin may fluidize the complete lipid matrix. This finding may be explained in terms of a strong hydrophilic interaction of the protein head group with the lipid-water interface. Such an effective lipid-protein interaction has already been demonstrated recently by freeze-fracture electron microscopy and by energy-transfer experiments (26). In this work it was also shown that the main transition temperature, T_m, of DMPC is depressed by addition of very small amounts of glycophorin. A phase diagram of the DMPC/glycophorin mixture was drawn, which exhibits some similarity to Fig. 4.

The observed fluidization of the lipid bilayer by glycophorin molecules has already been concluded from ^{13}C-NMR (41) and from electron microscopy (42) experiments. Very recently Posch et al. (43) reported a fluidization of phosphatidylcholine bilayers by small amounts of the bee venom peptide melittin. These authors discussed their results in terms of a phospholipid cluster model whereby one melittin molecule fluidizes a complete cluster in the $P_{\beta'}$ phase via long-range lattice disordering effects.

Glycophorin Diffusion and Lipid Protein Interaction

The lateral diffusion coefficient of glycophorin measured at low protein concentration (C_P < 0.5 mmol) and above

the lipid main transition amounts to $D_P = (4 \pm 1.5) \times 10^{-8}$ cm^2/s and is comparable with the lipid diffusion [$D_L = (5 \pm 1.5) \times 10^{-8}$ cm^2/s]. This result is consistent with an earlier work by Smith et al., in which it was found that the antibody bound to haptenated lipid diffuses as fast as the lipid itself (44). However, it is astonishing in view of our finding that one glycophorin molecule may bind rather strongly to some hundred lipid molecules. According to the hydrodynamic Saffman-Delbrück-Model (45) the diffusion coefficient is proportional to the logarithm of the radius of the diffusing species. Nevertheless, one should expect a remarkable decrease in D_P if the protein/lipid aggregate diffuses as an entity. This discrepancy may be explained by assuming that the hydrophilic lipid-protein interaction is highly dynamic so that the association of the side groups of the protein head group with the lipid head groups is only short-lived.

In the $P_{\beta'}$ phase we have to consider again the lipid defect structure. The results are equivalent to the lipid diffusion in the presence of glycophorin. Increasing amounts of glycophorin now increases the fraction of fast-diffusing proteins in the $P_{\beta'}$ phase (e.g. Fig. 1 *A* and *B*). Our results are in accordance with results of Wu et al. (22) who reported in a photobleaching study a concentration-dependent increase of the peptide diffusion in the $P_{\beta'}$ phase in gramicidin-containing membranes. Again the ripple structure visualized by electron microscopy was partially disintegrated after addition of gramicidin (46). In comparison with the fluid L_α phase the diffusion coefficients of the lipid, D_L, and of the protein, D_P, exhibit marked differences in the $P_{\beta'}$ phase. Fig. 9 shows the dependencies of D_L and D_P for a glycophorin content of 0.2 mmol/mol lipid. At 15°C for example, the protein diffusion ($D_P = 5 \times 10^{-9}$ cm^2/s) is by about a factor of four slower than the lipid diffusion ($D_L = 2 \times 10^{-8}$ cm^2/s). This may be interpreted in terms of a stronger hydrophilic lipid-protein interaction in the $P_{\beta'}$ phase as compared with the L_α phase. The adsorption of the sugar-containing protein head group to the lipid-water interface may thus have a longer lifetime in the crystalline phase. Another possible explanation is a steric hindrance of the protein diffusion in the fluid channels caused by bulky peptide-oligosaccharide head group of the protein, which sticks out into the water phase.

Another remarkable difference between lipid and protein diffusion in the $P_{\beta'}$ phase is observed with respect to the reversibility of the D vs. T plots. The curve for the lipid (Fig. 3 *A* and *B*) is fully reversible at increasing and decreasing temperature, whereas that for the protein exhibits a pronounced hysteresis. This may also be explained in terms of the formation of lipid-protein complexes. The formation of such complexes at low temperature ($T < 10$°C) has indeed been observed by electron microscopy (26).

Finally, we consider our results in the light of a recent theory on protein diffusion and lipid-protein interaction. A so-called icebreaker effect was postulated to explain protein lateral diffusion (42, 47). The theory assumes that the protein induces a local melting, which leads to the formation of a halo of fluid lipid around the protein. Such a model could not explain our observation of simultaneously fast and slowly diffusing glycophorin molecules because there is no reason to assume that only part of the glycophorin molecules would exhibit an icebreaker effect. Our results show instead that the glycophorin in DMPC should be considered as a binary mixture, which exhibits the lateral-phase separation already at very low protein concentrations ($C_P < 0.4$ mmol/mol lipid) that is induced by a substantial hydrophilic lipid-protein interaction.

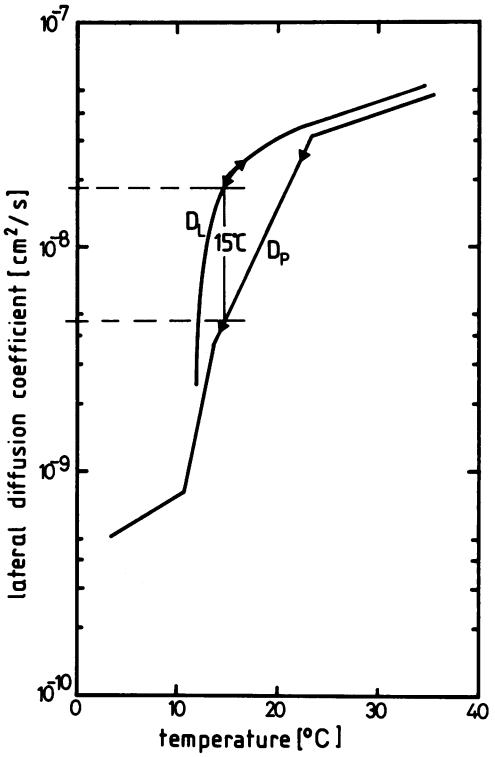

FIGURE 9 Comparison of the temperature dependence of the lateral diffusion coefficients of a lipid (NBD-PE) and a protein (glycophorin) in DMPC bilayers. The NBD-PE concentration was 0.5 mmol/mol lipid; the glycophorin concentration was 0.2 mmol/mol lipid in both preparations. Only the cooling curves are shown.

We are grateful to Professor Dr. P. Fromherz who made it possible for us to perform our experiments in the Department of Biophysics at the University of Ulm. We would like to thank U. Theilen for skilled technical assistance. Dr. Galla wishes to acknowledge a stimulating discussion with Dr. P. Laggner from the Akademie der Wissenschaften in Graz, Austria.

This work was supported by grants from the Deutsche Forschungsgemeinschaft under contracts no. Ga 233 and Sa 246.

Received for publication 29 November 1982 and in final form 27 June 1983.

REFERENCES

1. Cherry, R. J. 1979. Rotational and lateral diffusion of membrane proteins. *Biochim. Biophys. Acta.* 559:289–327.

2. Strittmatter, W. J., and M. J. Rogers. 1975. Apparent dependence of interactions between cytochrome b_5 and cytochrome b_5 reductase upon translational diffusion in dimyristoyl lecithin liposomes. *Proc. Natl. Acad. Sci. USA.* 72:2658–2661.
3. Fisher, R. W., and T. L. James. 1978. Lateral diffusion of the phospholipid molecule in dipalmitoylphosphatidylcholine bilayers. An investigation using nuclear spin-lattice relaxation in the rotating frame. *Biochemistry.* 17:1177–1183.
4. Lindblom, G., H. Wennerström, G. Arvidson, and B. Lindmann. 1976. Lecithin translational diffusion studied by pulsed NMR. *Biophys. J.* 16:1287–1296.
5. Deveaux, P., and H. M. McConnell. 1972. Lateral diffusion in spin-labelled phosphatidylcholine multilayers. *J. Am. Chem. Soc.* 94:4475–4482.
6. Sackmann, E., and H. Träuble. 1972. Studies of the crystalline phase transition of lipid model membranes. *J. Am. Chem. Soc.* 94:4482–4510.
7. Galla, H.-J., and E. Sackmann. 1975. Chemically induced lipid phase separation in model membranes containing charged lipids: a spinlabel study. *Biochim Biophys. Acta.* 401:509–529.
8. Galla, H.-J., and E. Sackmann. 1974. Lateral diffusion in the hydrophobic region of membranes: use of pyrene excimers as optical probes. *Biochim. Biophys. Acta.* 339:103–115.
9. Naqvi, K. R., J.-P. Behr, and D. Chapman. 1974. Methods for probing lateral diffusion of membrane components: triplet-triplet-annihilation of triplet-triplet energy transfer. *Chem. Phys. Lett.* 26:440–443.
10. Galla, H.-J., W. Hartmann, U. Theilen, and E. Sackmann. 1979. On two-dimensional passive random walk in lipid bilayers and fluid pathways in biomembranes. *J. Membr. Biol.* 48:215–236.
11. Galla, H.-J., and W. Hartmann. 1980. Excimer forming lipids in membrane research. *Chem. Phys. Lipids.* 27:199–219.
12. Webb, W. W. 1976. Applications of fluorescence correlation spectroscopy. *Q. Rev. Biophys.* 9:49–68.
13. Elson, E. L., and D. Madge. 1974. Fluorescence correlation spectroscopy. I. Conceptual basis and theory. *Biopolymers.* 13:1–27.
14. Fahey, P. F., D. E. Koppel, L. S. Barak, D. E. Wolf, E. L. Elson, and W. W. Webb. 1977. Lateral diffusion in planar lipid bilayers. *Science (Wash. DC).* 195:305–306.
15. Koppel, D. E. 1974. Statistical accuracy in fluorescence correlation spectroscopy. *Phys. Rev.* 10:1938–1945.
16. Vaz, W. L. C., Z. Derzko, and K. A. Jacobson. 1982. Photobleaching measurements of the lateral diffusion of lipids and proteins in artificial phospholipid bilayers membranes. *Cell Surf. Rev.* 8:83–136.
17. Wu, E. S., K. Jacobson, and D. Papahadjopoulos. 1977. Lateral diffusion in phospholipid multilayers measured by fluorescence recovery after photobleaching. *Biochemistry.* 16:3936–3941.
18. Smith, B. A., and H. M. McConnell. 1978. Determination of molecular motion in membranes using periodic pattern photobleaching. *Proc. Natl. Acad. Sci. USA.* 75:2759–2763.
19. Rubenstein, J. L. R., B. A. Smith, and H. M. McConnell. 1979. Lateral diffusion in binary mixtures of cholesterol and phosphatidylcholines. *Proc. Natl. Acad. Sci. USA.* 76:15–18.
20. Derzko, Z., and K. Jacobson, 1978. Lateral diffusion of a myelin membrane protein incorporated into phospholipid multivilayers. *Biophys. J.* 21(2 Pt. 2):234*a*. (Abstr.)
21. Vaz, W. C. C., K. Jacobson, E. S. Wu, and Z. Derzko. 1979. Lateral mobility of an amphipathic apolipoprotein, Apo C-III, bound to phosphatidylcholine bilayers with and without cholesterol. *Proc. Natl. Acad. Sci. USA.* 76:5645–5649.
22. Wu, E. S., K. Jacobson, F. Szoka, and A. Portis. 1978. Lateral diffusion of a hydrophobic peptide, *N*-4-nitrobenzo-2-oxa-1,3-diazole gramicidin S, in phospholipid multibilayers. *Biochemistry.* 16:3936–3941.
23. Wu, E. S., and C. S. Yang. 1980. Lateral diffusion of cytochrome P-450 in phospholipid multilayers. *Fed. Proc.* 39:1990. (Abstr.)
24. Wu, E. S., P. S. Low, and W. W. Webb. 1981. Lateral diffusion of glycophorin reconstituted into phospholipid multibilayers. *Biophys. J.* 33(2, Pt. 2):109*a*. (Abstr.)
25. Wey, C. L., R. A. Cone, and M. A. Edidin. 1981. Lateral diffusion of rhodopsin in photoreceptor cells measured by fluorescence photobleaching and recovery. *Biophys. J.* 33:225–232.
26. Rüppel, D., H. G. Kapitzka, H.-J. Galla, F. Sixl, and E. Sackmann. 1982. On the microstructure and the phasediagram of dimyristoylphosphatidylcholine-glycophorin bilayers. The role of defects and the hydrophilic lipid-protein-interaction. *Biochim. Biophys. Acta.* 692:1–17.
27. McDonald, R. I., and R. C. McDonald. 1975. Assembly of phospholipid vesicles bearing sialoglycoprotein from erythrocyte membrane. *J. Biol. Chem.* 250:9206–9214.
28. Vaz, W. L. C., H. G. Kapitza, J. Stümpel, E. Sackmann, and Th. M. Jovin. 1981. Translational mobility of glycophorin in bilayer membranes of dimyristoylphosphatidylcholine. *Biochemistry.* 20:1392–1396.
29. Peters, R., J. Peters, K. H. Tews, and W. Bähr. 1974. A microfluorometric study of translational diffusion in erythrocyte membranes. *Biochim. Biophys. Acta.* 367:282–294.
30. Axelrod, D., D. E. Koppel, J. Schlessinger, E. L. Elson, and W. W. Webb. 1976. Mobility measurement by analysis of fluorescence photobleaching recovery kinetics. *Biophys. J.* 16:1055–1069.
31. Kapitza, H. G., and E. Sackmann. 1981. Local measurement of lateral motion in erythocyte membranes by photobleaching technique. *Biochim. Biophys. Acta.* 595:56–64.
32. Rüppel, D. 1982. Zur Struktur von Phosphatidylcholindoppelschichten: Phasen, Defekte und Wechselwirkungen mit einem amphiphatischen Glycoprotein. Ph.D. thesis, University of Ulm. Ulm, Federal Republic of Germany.
33. Sackmann, E., D. Rüppel, and C. Gebhardt. 1981. Defect structure and texture of isolated bilayers of phospholipids and phospholipid mixtures. *Springer Ser. Chem. Phys.* 11:309–326.
34. Smith, L. M., J. L. R. Rubenstein, J. W. Parce, and H. M. McConnell. 1980. Lateral diffusion of M-13 coat protein in mixtures of phosphatidylcholine and cholesterol. *Biochemistry.* 19:5907–5911.
35. Galla, H.-J., and E. Sackmann. 1974. Lateral mobility of pyrene in model membranes of phospholipids with different chain length. *Ber. Bunsen-Ges. Phys. Chem.* 78:949–953.
36. Derzko, Z., and K. Jacobson. 1980. Comparative lateral diffusion of fluorescent lipid analogues in phospholipid multibilayers. *Biochemistry.* 19:6050–6057.
37. Lee, A. G. 1975. Fluorescence studies of chlorophyll, an incorporated into lipid mixtures, and the interpretation of "phase" diagrams. *Biochim. Biophys. Acta.* 413:11–23.
38. Lee, A. G. 1977. Analysis of the defect structure of gel-phase lipid. *Biochemistry.* 16:835–841.
39. Verkleij, A. J., P. H. J. Ververgaert, L. L. M. Van Deenen, and P. F. Elbers. 1972. Phase transitions of phospholipid bilayers and membranes of Acholeplasma Laidlawii B visualized by freeze fracturing electron microscopy. *Biochim. Biophys. Acta.* 288:326–332.
40. Falkowitz, M. S., M. Seul, H. L. Frisch, and H. M. McConnell. 1982. Theory of periodic structures in lipid bilayer membranes. *Proc. Natl. Acad. Sci. USA.* 79:3918–3921.
41. Brûlet, P., and H. M. McConnell. 1976. Protein-lipid interactions: glycophorin and dipalmitoylphosphatidylcholine. *Biochem. Biophys. Res. Commun.* 68:363–368.
42. Grant, Ch. W. M., and H. M. McConnell. 1974. Glycophorin in lipid bilayers. *Proc. Natl. Acad. Sci. USA.* 71:4653–4657.
43. Posch, M., U. Rakusch, Ch. Mollay, and P. Laggner. 1983. Cooperative effects in the interaction between melittin and phosphatidylcholine model membranes. Studies by temperature scanning densitometry. *J. Biol. Chem.* 258:761–766.
44. Smith, L. M., J. W. Parce, B. A. Smith, and H. M. McConnell. 1979.

Antibodies bound to lipid haptens in model membranes diffuse as rapidly as the lipids themselves. *Proc. Natl. Acad. Sci. USA.* 76:4177–4179.

45. Saffmann, P. G., and M. Delbrück. 1975. Brownian motion in biological membranes. *Proc Natl. Acad. Sci. USA.* 72:3111–3113.
46. Chapman, D., B. A. Cornell, A. W. Eliasz, and A. Perry. 1977. Interactions of helical polypeptide segments which span the hydrocarbon region of lipid bilayers. Studies of the gramicidin a-lipid-water-system. *J. Mol. Biol.* 113:517–538.
47. Pink, D. A., T. Lookman, L. McDonald, M. J. Zuckermann, and N. Jan. 1982. Lateral diffusion of gramicidin S, M-13 coat protein and glycophorin in bilayers of structural phospholipids. Meanfield and Monte Carlo studies. *Biochim Biophys. Acta.* 687:42–56.